Some remarks on the micromechanical modeling of glass/epoxy syntactic foams

by

Lorenzo Bardella and Francesco Genna

ABSTRACT

We focus on the continuum micromechanics of syntactic foams constituted by epoxy matrix and glassy filler. Such ingredients are often privileged for engineering applications since they both provide good properties for the final composite and best meet the technological requirements in the manufacturing stage [1].

In particular, we wish to analyze both the behavior under cyclic loads and the brittle failure of some peculiar syntactic foams under uniaxial, compressive loading conditions.

The analysis, which resorts to both analytical and numerical techniques, shows that the mechanical behavior of syntactic foams is strongly affected by the filler density ρ_f, directly related to the following average of the ratio between the inner and outer radii of the whole population of cenospheres, i.e., the "radius ratio" η (as called in [2]):

$$\eta = \sqrt[3]{1 - \frac{\rho_f}{\rho_g}} \tag{1}$$

in which ρ_g is the glass density.

Moreover, it is evicted that the failure, at least when brittle, must also depend on the size of the filler particles, usually cenospheres whose outer diameter measures a few tens of microns.

The simulations are validated by comparison with experimental results available in the literature.

Department of Civil Engineering, University of Brescia, via Branze, 38, 25123 Brescia, Italy.

INTRODUCTION

Syntactic foams can be designed, at least with regard to their stiffness, by means of analytical homogenization techniques [3], while the use of numerical methods can help in obtaining useful informations about their nonlinear and inelastic behavior.

Here, we wish to get an insight into the influence of the radius ratio η, as defined by equation (1), on the effective stiffness and strength of these composites.

The experiments carried out by De Runtz and Hoffman [4], Bardella [5], Rizzi et al. [6], and Gupta et al. [2] have allowed recognition of different failure modalities in the uniaxial compression of glass/epoxy syntactic foams.

For instance, for a sufficiently heavy filler, with volume fraction higher than 50% and no much air bubbles entrapped into the matrix in the manufacturing stage (henceforth called "unwanted voids"), cylindrical specimens fail in a small displacement regime by fracturing along planes including the loading axis ([5], [2]).

Instead, for higher particle contents, usually accompanied by a not negligible presence of unwanted voids, and for lower filler densities (i.e., higher η), the failure exhibits shear bands inclined at 45° with respect to the load direction [6].

Owing to the difficulty at defining and implementing an accurate model for the prediction of failure in the resin matrix, which can not be neglected, in general, among the causes of crisis for the syntactic foams in the second and other cases, here we are concerned with the former case only, for which it may be conjectured that the failure is likely to be triggered off by micro-defects existing in the filler, when the matrix can still bear stresses.

In order to follow a micromechanical approach, we need models for the behavior of the single composite phases. Here, the glass behavior is taken as linear elastic, whereas the epoxy resin pre-yield behavior is described by a nonlinear viscoelastic constitutive law developed in [7]. Filler and matrix are assumed to be perfectly bonded, also in view of the nowadays customary glass silanization process.

The uniaxial compression of a particular syntactic foam is then studied by coupling analytical homogenization techniques and numerical models, the former being available in the literature ([5], [3], and [8]) and summarized in the next section.

A THEORETICAL HOMOGENIZATION PROCEDURE

The Linear Elastic Homogenization Procedure (LEHP)

"Classical" LEHPs are ineffective in either bounding or estimating the elastic moduli of syntactic foams. This is because these LEHPs can not simultaneously account for both the connectedness of the matrix and the peculiar structure of the cenospheres. However, it is possible to develop quite accurate LEHPs for these composites by exploiting the Morphologically Representative Pattern theory [9] and by assuming that the Representative Volume Element (RVE) be a Composite Sphere Assemblage [10]. The LEHP here summarized somehow extends that of Hervé and Pellegrini [11], in that it can estimate the elastic moduli of syntactic foams in which there is the need to account for a graded filler and for the presence of unwanted voids. In this LEHP, the local fields in any different composite sphere are evaluated by means of Eshelby-like problems consisting of four–phase models, subjected to proper boundary conditions, such as those sketched in figure 1 (in which $S1$ and $S2$ indicate two different composite spheres related to cenospheres of different heaviness, whereas SM stands for the composite sphere taking the unwanted voids into account. Each of the M types λ of composite spheres, needed in order to describe the composite morphology, is characterized by the ratio a_λ/b_λ between the inner and the outer radii of the considered cenosphere, of known volume fraction f_λ with respect to the sole filler ($\sum_{\lambda=1}^{M} f_\lambda = 1$). $f_\lambda f$ is then the volume fraction of the filler accounted for by the composite sphere λ into the syntactic foam, f being the overall filler volume fraction. The outer radius c_λ defining the external matrix shell of a composite sphere depends on f in such a way that $c_\lambda = b_\lambda/f^{1/3}$. Should there be the need to take unwanted voids into account, it is sufficient to consider a special four–phase model (actually collapsing into a three–phase model) whose composite sphere is characterized by the choice $a_\lambda = b_\lambda$.

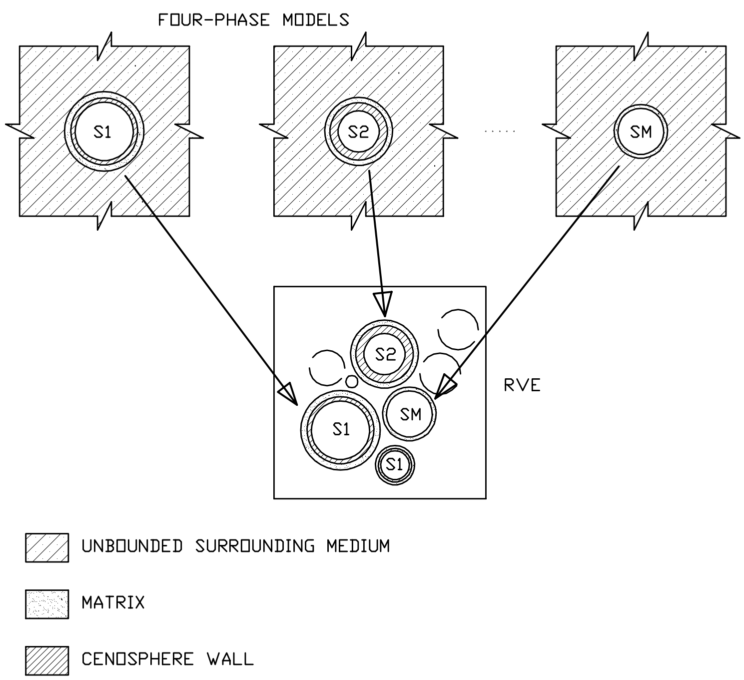

Figure 1. The four-phase models and the Composite Sphere Assemblage.

The effective shear and bulk moduli, G_0^{est} and K_0^{est}, of syntactic foams can then be computed by means of the following relations, coupled if more than one composite sphere are considered:

$$G_0^{est} = \frac{\displaystyle\sum_{\lambda=1}^{M} f_\lambda \Big\{ G_\lambda^{(i)} f \Big[1 - \Big(\frac{a_\lambda}{b_\lambda} \Big)^3 \Big] \overline{\varepsilon}_{12}^{(i),\lambda} + G_\lambda^{(m)} (1-f) \overline{\varepsilon}_{12}^{(m),\lambda} \Big\}}{\displaystyle\sum_{\lambda=1}^{M} f_\lambda \overline{\varepsilon}_{12}^{(c.s.),\lambda}} \tag{2}$$

$$K_0^{est} = \frac{\displaystyle\sum_{\lambda=1}^{M} f_\lambda \Big\{ K_\lambda^{(i)} f \Big[1 - \Big(\frac{a_\lambda}{b_\lambda} \Big)^3 \Big] \overline{\vartheta}^{(i),\lambda} + K_\lambda^{(m)} (1-f) \overline{\vartheta}^{(m),\lambda} \Big\}}{\displaystyle\sum_{\lambda=1}^{M} f_\lambda \overline{\vartheta}^{(c.s.),\lambda}} \tag{3}$$

in which $G_\lambda^{(i)}$, $K_\lambda^{(i)}$, $G_\lambda^{(m)}$, and $K_\lambda^{(m)}$ are the elastic moduli of the (isotropic) inclusion wall and the (isotropic) matrix of the composite sphere λ, and $\overline{\varepsilon}_{12}^{(i),\lambda}$, $\overline{\vartheta}^{(i),\lambda}$, $\overline{\varepsilon}_{12}^{(m),\lambda}$, $\overline{\vartheta}^{(m),\lambda}$, $\overline{\varepsilon}_{12}^{(c.s.),\lambda}$, and $\overline{\vartheta}^{(c.s.),\lambda}$ are strain averages over the inclusion wall, the matrix, and the whole composite sphere, to be computed by means of the systems provided in appendix. The fact that $G_\lambda^{(m)}$ and $K_\lambda^{(m)}$, may be different for each λ is due, in view of extending this technique to the nonlinear range, to the change in the local matrix stiffness consequent upon the strain growth, whereas the dependence of $G_\lambda^{(i)}$ and $K_\lambda^{(i)}$ on λ may even ensue from the use of many fillers, each made up of a different material.

Depending on the chosen elastic moduli $G^{(s)}$ and $K^{(s)}$ of the unbounded surrounding medium in the four–phase models, it is possible to obtain the corresponding of all the "classical" estimates and bounds, now said "composite sphere–based".

In particular, if $G^{(s)}$ and $K^{(s)}$ take the values of the matrix we have the Mori–Tanaka "composite sphere–based" estimate, while assigning to $G^{(s)}$ and $K^{(s)}$ the unknown effective values of the composite provides the Self–Consistent "composite sphere–based" estimate, which, even though it requires the solution of a nonlinear algebraic problem, will be always exploited in the following analyses being the most accurate. In this case, it turns out that the homogeneous kinematic boundary conditions applied to the RVE, governed by the constant strain tensor E_{ij}, are exactly the same as those applied to each four-phase model.

AN APPLICATION: THE EFFECT OF η ON THE EFFECTIVE MODULI

Based on the above LEHP, we investigate the dependence of the elastic moduli on the filler heaviness, as represented by the radius ratio η.

We focus on syntactic foams, with no unwanted voids, constituted by the epoxy resin DGEBA DER 332, produced by Dow Chemicals, cured with the hardener DDM Fluka 32950, and filled, for a fixed volume fraction $f = 0.515$, with glass cenospheres produced by 3M Italia [12] and called "Scotchlight^{TM} Glass Bubbles", or "microballoons". The epoxy Young's modulus, Poisson's ratio, and density respectively read E_e=2800 MPa, ν_e=0.41, and ρ_e=1.18 g/cm^3, whereas for the glass we assume E_g=77500 MPa, ν_g=0.23, and ρ_g=2.60 g/cm^3 (for a discussion on these data, see [5]).

Bardella [5] provides the experimental data related to two syntactic foams of this kind, henceforth called "syntactic foam type A" and "syntactic foam type B". They are respectively filled with K37 and H50 microballoons, the former of density ρ_f=0.37 g/cm^3 corresponding to η=0.9501, whereas for the latter ρ_f=0.5 g/cm^3 and, then, η=0.9313. It has been shown that the filler gradation can be neglected in the computation of the effective moduli of these particular composites ([5] and [3]).

Figures 2 and 3 report the representative experimental results for these two syntactic foams together with the theoretical predictions for a continuously variable η. The results are shown in terms of Young's and shear moduli as functions of the composite density,

$$\rho_{sf} = (1-f)\rho_e + f(1-\eta^{\ 3})\rho_g \tag{4}$$

computed for all the possible values $\eta \in$ [0,1]. It is important to note that when η is close to 1 (i.e., the case of interest in the applications) a little change in its value has quite a large influence on both the effective moduli and density. On the contrary, when η is close to zero its variation produces little changes both on the elastic moduli

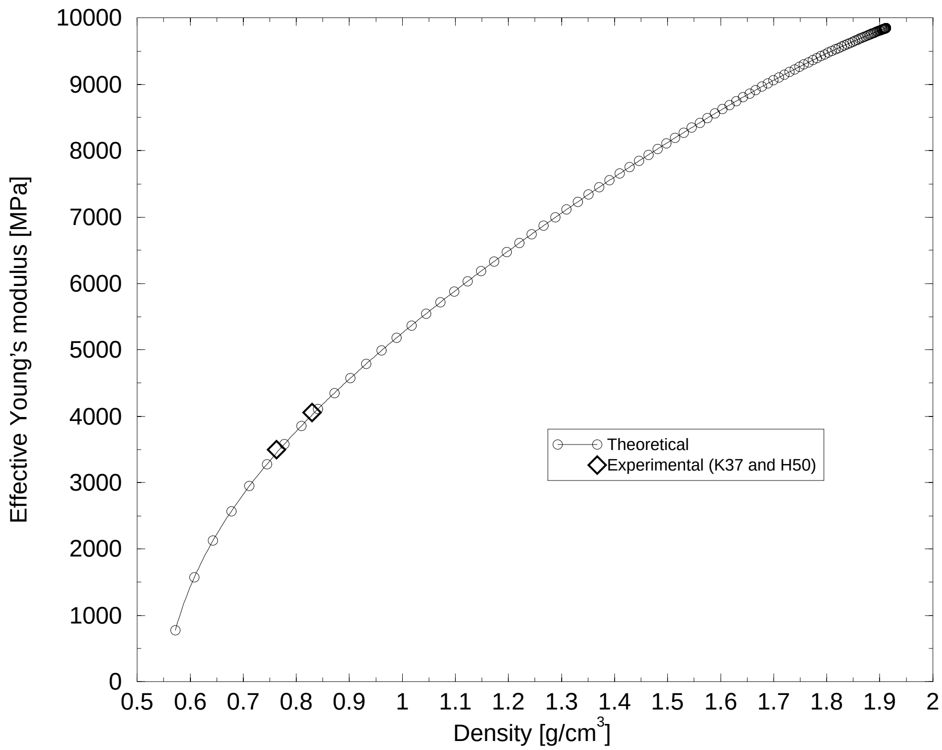

Figure 2. Effective Young's modulus versus composite density.

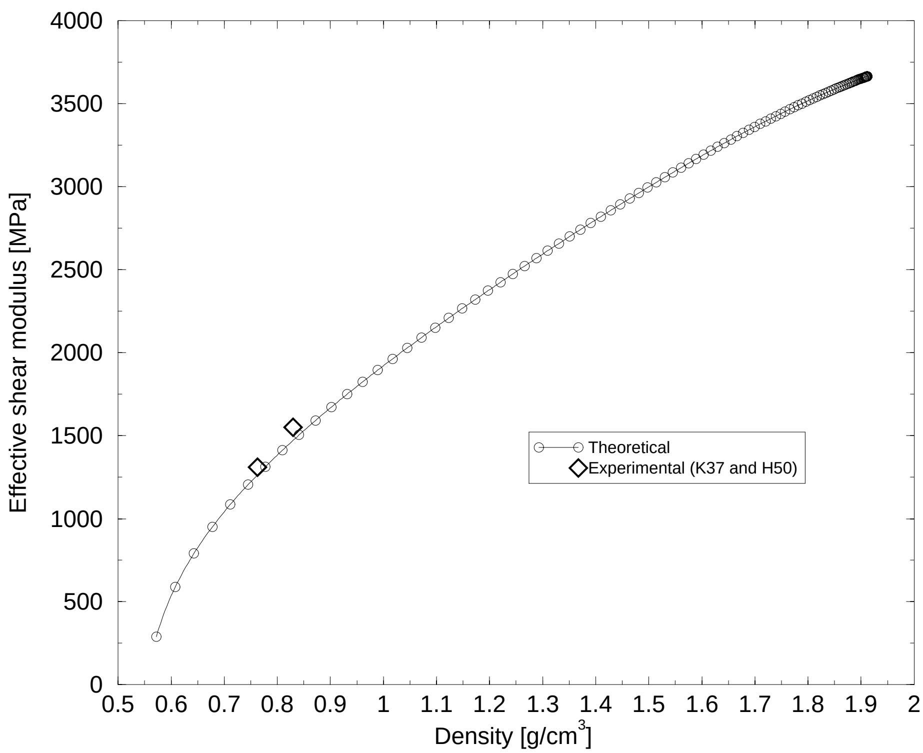

Figure 3. Effective shear modulus versus composite density.

and on the density; this is the reason why the slope in the moduli-density curves is still quite significant also for high values of the effective density.

An Efficient Extension Beyond the Linear Elastic Range

By following the approach reviewed by Suquet [3], in order to extend any LEHP to the nonlinear range one just needs to be able to compute the current stiffness of each phase in the RVE subjected to some loading path. This can be accomplished by having a suitable constitutive law for each phase and, most of all, by being able to evaluate a proper average of the local strain over each phase.

The constitutive law for the epoxy matrix exploited in the analytical homogenization in this work is nonlinear only by the following invariant of the the local strain field ε_{ij} computed through the "composite sphere–based" LEHP over each four-phase model:

$$\varepsilon_{eq} = \sqrt{\frac{2}{3} e_{ij} e_{ij}} \tag{5}$$

where $e_{ij} = \varepsilon_{ij} - \vartheta\delta_{ij}$ and $\vartheta = \varepsilon_{kk}/3$. Hence, we provide the formulæ to compute the second-order average of ε_{eq}, say $\overline{\overline{\varepsilon}}_{eq}$. The results for $\overline{\overline{\vartheta}}$ are given in [8].

Using this kind of second-order averages to evaluate the local stiffness constitutes the Extended Secant Method, a method particularly efficient for syntactic foams and alternative to Suquet's Second Order Secant Method, which instead indirectly exploits the real local field in the RVE [8].

The results reported in the following can be used for any particulate composite filled with multilayered spherical inclusions; in particular, as for the related LEHP previously summarized, they can be straightforwardly adapted to the case in which the effect of an interphase (for instance due to the filler silanization [14]) between matrix and cenospheres has to be accounted for.

The linear elastic solution on the generic spherical shell (i.e., the layer) has the same form as that in the matrix shell in the four-phase model for syntactic foams, and it depends on six coefficients ($P_1, P_2, M_1, M_2, M_3, M_4$ according to the notation adopted in appendix) to be determined by solving a boundary value problem. We will refer the formulæ to the matrix shell in syntactic foams.

The local strain field, ε_{ij}, due to kinematic homogeneous boundary conditions applied to the four–phase model is given in [5] and [8]. By representing the constant strain tensor E_{ij} governing the boundary conditions as the superposition of its simple shear components (Φ_{12}, Φ_{23}, and Φ_{31}) and its spherical part $\Theta = E_{kk}/3$, we have

$$\overline{\overline{\varepsilon}}_{eq}^{(m)} = \sqrt{S_{\varepsilon_{eq}} {E_{eq}}^2 + B_{\varepsilon_{eq}} \Theta^2} \tag{6}$$

in which $S_{\varepsilon_{eq}}$ depends only on the simple shear boundary conditions, whereas $B_{\varepsilon_{eq}}$ is related to Θ:

$$\begin{aligned} S_{\varepsilon_{eq}} = {} & M_1^2 + \frac{6a^{10}(c^7 - b^7)}{b^7 c^7 (c^3 - b^3)} M_2^2 + \frac{2(c^5 - b^5)}{5a^2(c^3 - b^3)}(5 + \alpha_2^{(m)}) M_1 M_3 + \\ & + \frac{c^7 - b^7}{210 a^4 (c^3 - b^3)}(278 + 128\alpha_2^{(m)} + 17{\alpha_2^{(m)}}^2) M_3^2 + \frac{12 a^8 (c^5 - b^5)}{5 b^5 c^5 (c^3 - b^3)}(5 - \alpha_{-3}^{(m)}) M_2 M_4 + \\ & - \frac{a(c^2 - b^2)}{10(c^3 - b^3)}(2 + \alpha_2^{(m)})(2 + \alpha_{-3}^{(m)}) M_3 M_4 + \frac{a^6}{10 b^3 c^3}(72 - 28\alpha_{-3}^{(m)} + 3{\alpha_{-3}^{(m)}}^2) M_4^2 \end{aligned} \tag{7}$$

$$B_{\varepsilon_{eq}} = \frac{4a^6}{b^3c^3}P_2^2 \tag{8}$$

and

$$E_{eq} = \sqrt{\frac{2}{3}\mathcal{E}_{ij}\mathcal{E}_{ij}} = \sqrt{\frac{4}{3}({\Phi_{12}}^2 + {\Phi_{23}}^2 + {\Phi_{31}}^2)} \qquad \mathcal{E}_{ij} = E_{ij} - \Theta\delta_{ij} \tag{9}$$

In the expressions above the constants P_2, M_1, M_2, M_3, and M_4 have to be computed from the systems reported in appendix in which $\Phi = 1$ and $\Theta = 1$. Moreover, we have omitted the symbol λ even though the above equations must be solved for each composite sphere.

We emphasize that $\overline{\overline{\varepsilon}}_{eq}^{(m)}$ depends on both E_{eq} and Θ, that is what one might expect, for, by the way, it means that the effective volumetric behavior can be nonlinear even though the bulk behavior of all the phases is linear elastic, and this agrees with well known analogous results which can be found in the context of linear viscoelasticity by means of the “exact” Correspondence Principle.

In [8] a very simple nonlinear elastic model for the epoxy resin has been adopted in order to check the (satisfactory) predictive capability of the homogenization technique here summarized for monotonic loading conditions and for the specific range of strain rates involved in the experimental tests considered.

In general, any analytical homogenization technique beyond the linear elastic range suffers the need to employ very simple constitutive laws for each phase. Unfortunately, epoxy resins have a constitutive behavior governed by a rheology requiring sophisticated models in order to obtain an accurate prediction of their local response (e.g., [7]). Therefore, in the next section, to reach our goal we will resort to both analytical and numerical techniques. The former, based on the above mentioned simplified model for the matrix, will allow for a simple and efficient description of the interaction between different composite spheres, whereas the latter will provide the detailed stress field of a particular composite sphere.

ON THE UNIAXIAL COMPRESSIVE STRENGTH

Here, we wish to give ground to the conjecture that under uniaxial compression the failure of glass/epoxy syntactic foams may happen since the microballoons act as sources for crack initiation [15]. Also, we shall evict that the distribution of the cenosphere ratio a_λ/b_λ may play an important role in the failure behavior.

From the continuum micromechanics viewpoint, the prediction of the strength of syntactic foams constitutes a very difficult task, for it depends upon many parameters, such as the material behavior of the phases, the microstructure, and the macroscopic boundary conditions applied. The microstructure, in turn, is an aleatory parameter usually expressed for syntactic foams just by means of the filler volume fraction, the filler density (related to η by equation (1)), and, if it is the case, the presence of unwanted voids.

Comments on some Experimental Results

A first insight into the strength of glass/epoxy syntactic foams has been given in the pioneering work of De Runtz and Hoffman [4]. More recently, other results have been obtained by Rizzi et al. [6], Bardella [5], and Gupta et al. [2]. We consider only the compressive strength of syntactic foams with very high filler volume fraction (always higher than 50%), that is of course the most interesting engineering case.

In this case, to the authors knowledge, so far the following four failure modalities have been observed:

1. splitting along planes including the loading direction (uniaxial compression, brittle fracture. See figure 4 from Bardella [5] and see Gupta et al. [2]);

2. 45° inclined shear bands (uniaxial compression, quasi-brittle fracture. Rizzi et al. [6]);

3. crushing of a localized "weak layer" perpendicular to the loading direction (uniaxial compression. De Runtz and Hoffman [4]);

4. large-scale breakage of inclusions with no macroscopic fracture and large amount of inelastic deformations (uniform volumetric loading and other loading conditions with prevalent compression. De Runtz and Hoffman [4]).

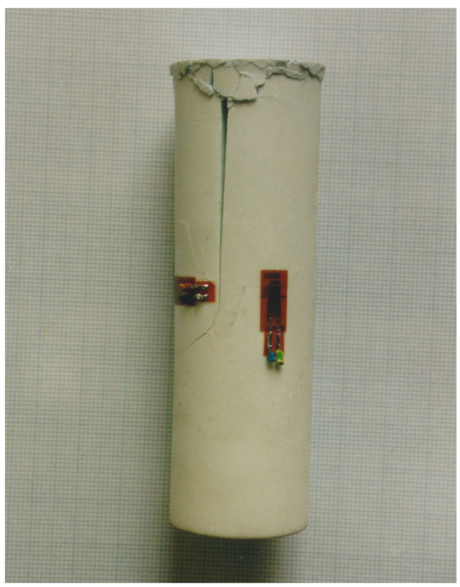

Figure 4. The failure modality type 1 on the syntactic foam type A.

The analysis of the materials tested by De Runtz and Hoffman [4], Rizzi et al. [6], Bardella [5], and Gupta et al. [2] allows the conjecture that these four types of failure modality are related to the filler heaviness, i.e., the radius ratio η.

In particular, the above reported failure modalities are ordered as η of the tested composites.

In order to get an insight into which η may help discriminating among the above different failure modalities[1], let us now focus on the microstructure of the related syntactic foams.

Whereas the failure modality type 1 characterizes syntactic foams filled with quite heavy glass microballoons (i.e., fillers with not too high η), the second failure

[1] Gupta and Woldesenbet [16] conjecture that η=0.71 must discriminate between two completely different failure modalities, if related to microballoons breakage. Instead, our analysis tries and distinguish among different failure modalities occuring at much higher values of η.

modality listed above concerns lighter syntactic foams, and so on, as far as the fourth collapse description, inherent the lightest syntactic foams among those tested by De Runtz and Hoffman [4], Rizzi et al. [6], and Bardella [5]. Gupta et al. [2] tested, still under uniaxial compression, different syntactic foams containing unwanted voids, having density ranging from 0.493 g/cm^3 to 0.650 g/cm^3, and obtained by employing microballoons of different η (η=0.937$\div$0.973 for ρ_f=0.460 g/cm^3$\div$0.205 g/cm^3 having chosen ρ_g=2.6 g/cm^3) in a volume fraction of about 60%; by analyzing these experimental results Gupta and Woldesenbet [16] observed that the first type of failure modality is more prominent as η decreases.

Hence, the syntactic foams experiencing a failure modality of the type 1 are both syntactic foams types A and B, as described earlier and respectively characterized by $\eta = 0.9501$ and $\eta = 0.9313$, together with the heaviest among those tested by Gupta et al. [2].

The syntactic foam studied by Rizzi et al. [6] is instead made up of 3M's K1 microballoons embedded into the epoxy resin SP Ampreg 20^{TM} cured with UltraSlow Hardener (E_e=3700 MPa, ν_e=0.40); in this case ρ_f=0.125 g/cm^3, corresponding to η=0.9837. It is important to observe that the failure modality must depend on the relative stiffness of filler and matrix. Therefore, the effect of the extremely light filler employed in the syntactic foams tested by Rizzi et al. [6] is very likely emphasized by the fact that the matrix is quite stiff, also in comparison with the DGEBA DER 332 binder.

Similarly, the fact that Gupta et al. [2] observed failure modalities resembling the type 1 also for syntactic foams filled with quite light microballoons (η up to ≈ 0.97) can be explained with the relatively soft binder they employed ($E_e \approx 2320$ MPa).

The data provided by De Runtz and Hoffman [4] do not allow identification of the real filler density, also owing to the much likely presence of unwanted voids in their composites; anyway, their syntactic foams are extremely light, having a density ρ_{sf}=0.545$\div$0.785 g/cm^3.

The brittleness related to the different failure modalities types 1 and 2 under uniaxial compression is represented in figure 5. The dotted curve shows the behavior of the syntactic foam type A, whereas the dashed curve is taken from Maier [17] and is representative of the tests performed by Rizzi et al. [6], related to the failure modality type 2. The dot-dashed plot is the result of a test reported in [5] and carried out on a syntactic foam similar to that tested by Rizzi et al. [6], but filled with sifted K37 microballoons, having external diameter $2b_\lambda$=63 μm$\div$90 μm and η=0.953; the failure modality of this foam is unclear, likely being a mix of types 1 and 2.

Because of the high viscosity of epoxy resins, also the applied strain rate is an issue; unfortunately, in the tests represented in figure 5 it varies between 0.005 min^{-1} and 0.0375 min^{-1}. In spite of this, it can be evicted that the brittleness decreases as η increases.

In figure 6 we show the behavior we wish to model by means of continuum micromechanics. This figure shows stress-strain plots of uniaxial compressive tests preformed by Bardella [5] on both syntactic foams types A and B. The black plots are related to cyclic tests whereas the red ones concern monotonic loading up to brittle failure of type 1. The imposed strain rate is v=0.01 min^{-1}. Our modeling, for what concerns the failure, will focus on the syntactic foam type A.

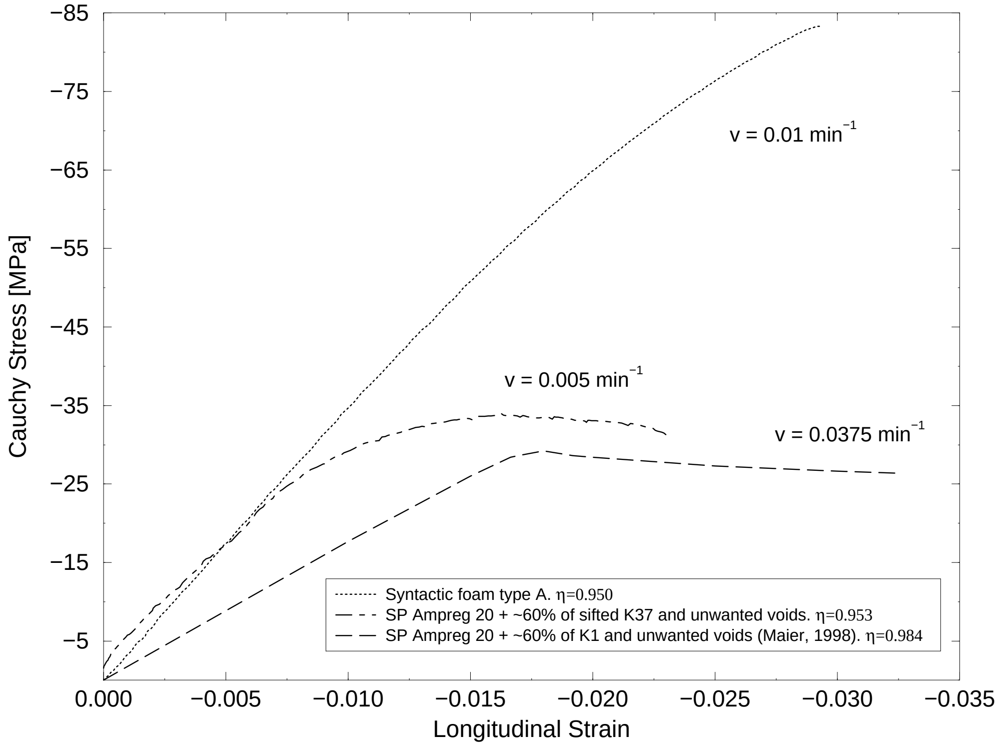

Figure 5. The uniaxial compressive behavior up to failure for different syntactic foams.

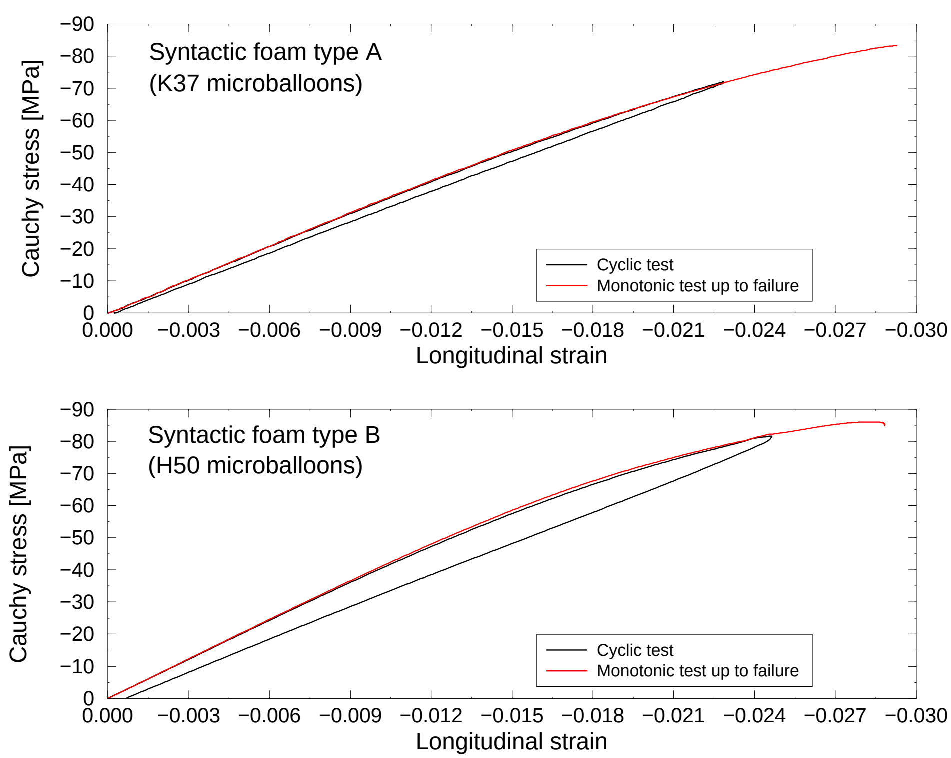

Figure 6. The results of uniaxial compressive tests on syntactic foams type A and type B.

Modeling the Incipient Failure

A PLANAR UNIT CELL MODEL

As shown in [7], the cyclic behavior represented in figure 6 may be described by making use of the Finite Element axisymmetric unit cell model depicted in figure 7, if a proper law for the epoxy matrix is available.

The uniaxial compressive tests are simulated by imposing uniform shortening displacement rates on the unit cell top and by suitably constraining the unit cell model to satisfy the periodicity condition (see figure 7). This model can only approximate the syntactic foams morphology since: (i) its cylindrical shape does not allow it to completely fill the space, (ii) syntactic foams we are random composites, and (iii) the real microballoons have variable size.

In order to describe the epoxy behavior before its strength is reached[2], in [7] it is proposed a nonlinear viscoelastic constitutive law based on a rheological model, called "Standard Linear Solid" in linear viscoelasticity, constituted by three elements in which a nonlinear spring of the Ramberg–Osgood type is put in parallel with a dashpot ruled by an Eyring law [18] extended to account for triaxial stress states; to such a "Kelvin-like model", a linear elastic spring describing the instantaneous response of the van der Waals intermolecular forces [19] is connected in series. In particular, this arrangement allows us to catch the peculiar flex in the unloading part of the stress-strain curve.

All the analyses have been run on the Finite Element code ABAQUS [20], in which the constitutive law for epoxy resins has been implemented in a "User Material" subroutine.

In figure 8, the experimental and the numerical results are compared. The match is quite satisfactory, even in terms of the unloading part. Beside the elastic moduli given above, the epoxy model requires other five material constants, as given in [7].

Once we know that the unit cell model can describe the mild nonlinearity of the syntactic foam type A before failure, the same model can also be employed in order to try and understand the reasons for failure of this syntactic foam. By subjecting the unit cell to the macroscopic boundary conditions up to failure as in the test (see the red plot in figure 6 for the syntactic foam type A), we observe (see the left picture in figure 9) that the highest local stress level is the hoop stress in the glass, of about 786 MPa, while the stress in the matrix (as represented by the restricted contours on the right in figure 9) is safely below the epoxy strength and then still in the viscoelastic range. This suggests that the crack might start propagating when the matrix has not yet reached its strength in any material point, and, then, that i) the constitutive model employed for the matrix, neglecting the post-yield behavior, is adequate to investigate the reason for this failure modality and ii) the stress component that triggers the crack propagation might be the hoop stress in the glass, fact which would explain the orientation of observed macro-cracks (figure 4).

Hence, at this point, we wish to establish whether there may exist a defect of sensible geometry and shape in the glass which propagates for a stress state corresponding to that obtained with the above unit cell analysis (mainly characterized by a tensile stress hoop stress of about 800 MPa). To this purpose we resort to Linear Elastic Fracture Mechanics.

[2] The experimental tests reported in [5] have shown that for this epoxy resin, as for many other polymers, the material strength can be assumed to coincide with the yield stress.

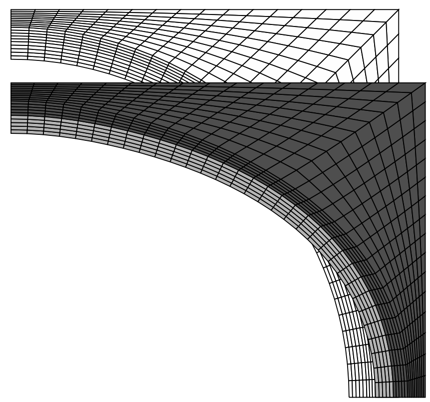

Figure 7. The axisymmetric unit cell and its deformed shape.

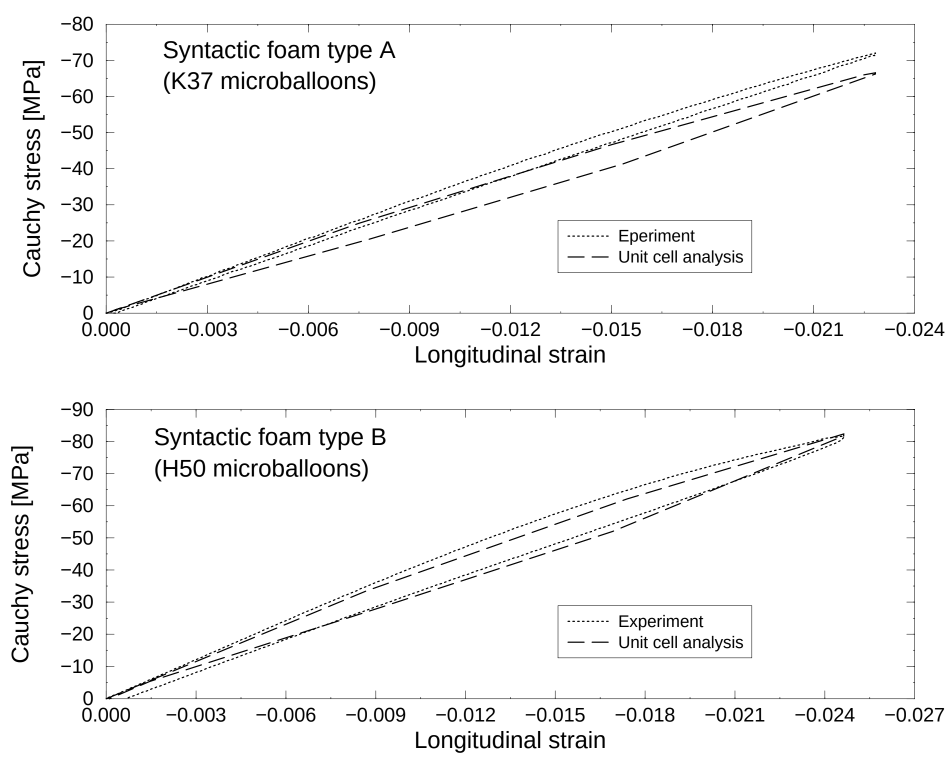

Figure 8. Cyclic behavior: the comparison between experimental and numerical results.

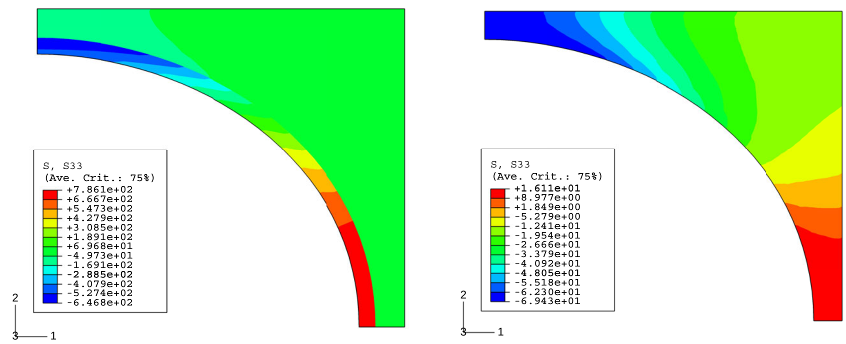

Figure 9. Axisymmetric unit cell model: the hoop stress contours at failure.

Note that Wei et al. [21] adopted a glass tensile strength of 700 MPa for similar microballoons, still filling an epoxy resin. Unfortunately, they did not justify the use of such a value, apart that it allowed fitting the experimental results.

A 3D ESHELBY-LIKE MODEL

As shown above, the planar unit cell model can predict the effective viscoelastic behavior of syntactic foams subjected to simple macroscopic boundary conditions. On the other hand, its capability to predict a peak in the local stress state must be corroborated by sound arguments. Then, first of all, we check the numerical predictions by removing some approximation inherent to the axisymmetric model. We then switch to a prismatic three-dimensional unit cell which can fill the space when repeated. The uniaxial macroscopic boundary conditions allow us to mesh just one twentyfourth of the whole unit cell. The relevant results, analogous to those reported in figure 9, are shown in figure 10 and indicate that the stress state predicted by the axisymmetric model is accurate enough.

Meshing a sensible defect into the glass, of course, requires to switch to a model able to describe the interaction between the cracked microballoon and its surrounding, the unit cell model being no longer appropriate.

Hence, we analyze the stress concentration on the crack front of a flawed microballoon into a syntactic foam by exploiting an Eshelby-like model, depicted in figure 11, in which a prismatic unit cell, consisting of a cracked cenosphere surrounded by a volume of matrix consistent with its volume fraction, is embedded into a very large volume of homogeneous material, whose stiffness is computed by exploiting the analytical nonlinear homogenization procedure summarized in the previous section. The symmetry conditions allow us to mesh just a quarter of the whole model.

Since the homogenization procedure exploited to assign, step-by-step, the current stiffness of the surrounding medium in the Eshelby-like model is nonlinear elastic (and rate-independent), the model is good only for monotonic loading conditions and for a given range of imposed strain rate. Such a range is dependent upon the modalities of the experimental tests whose results have been employed to identify the material parameters of the simplified epoxy model involved in the analytical homogenization [8].

Figure 11 also shows the shape of the chosen defect. It is a part-through crack of nearly semi-elliptical shape. Its depth, taken in the direction of the minor axis, is a quarter of the cenosphere wall thickness. The major axis is as long as twice the minor one. Of course, the flaw is oriented in such a way as to open when the syntactic foam is compressed, i.e., when the Eshelby-like model is subjected to uniform shortening displacements on its homogeneous face normal to the defect plane. Such a boundary condition has to mimic the one chosen in the experiment, so that the displacement in the model is imposed up to the corresponding effective strain equals the value at failure experimentally observed ($\approx$-0.03 and reached at a rate v=0.01 min^{-1}).

Moreover, note that, just for the sake of easy meshing, the flaw has been located on the inner side of the cenosphere wall. This might seem to be less probable than other choices, but, for the η value here considered it should not strongly affect the results.

This defect choice is arbitrary, but seems to be sensible since there should exist, among the whole population of microballoons in the syntactic foam, at least one flawed cenosphere whose defect is approximately oriented as here considered. Of course, under the same macroscopic boundary conditions, other flaws oriented in different ways are subjected to much less dangerous local stress states.

This model has been first of all run without enclosing any flaw, and it has been positively checked that the stress state in the hollow sphere is very similar to that provided by the unit cell analysis.

The main goal here is to check whether the stress intensity factor (SIF) distribution along the crack front somewhere reaches the glass fracture toughness value, K_C=0.7÷0.8 MN/m$^{1.5}$ [22].

Figure 12 shows, on the deformed shape, the stress singularity at the crack front in terms of the direct stress component normal to the crack faces (i.e., the hoop stress). The analysis has been run by means of the Finite Element code ABAQUS [20] and the SIF distribution evaluated by passing through the J-integral computation. As expected, the maximum SIF value is very close to K_C. In particular, we obtained K_I=0.78 MN/m$^{1.5}$. These results have been successfully checked also by running an analysis on a coarser mesh in which the 20-node brick elements on the crack front were implemented as quarter-point elements (see figure 13).

This analysis can then explain the reason for failure in the syntactic foam type A under uniaxial compression, at least for the considered loading rate. In fact, it seems that macroscopic failure is triggered by some defect in the glass, at the macroscopic longitudinal strain of -0.03 and stress of -85 MPa (that is, the “far-field stress”), due to mode I propagation of flaws subjected to dominant tensile hoop stress.

It is interesting to note that the ratio between the magnitudes of the local maximum tensile stress ($\approx$ 800 MPa) and the far-field stress ($\approx$ 85 MPa) is about 9, much higher than 3, corresponding to the similar ratio for the linear elastic problem in which the inclusion is just a spherical hole. The reasons for this amplification are obviously to be found in the particular syntactic foam microstructure (the glass is much stiffer than epoxy, so that it draws stresses), but also the epoxy viscoelastic behavior plays an important role in transferring self-equilibrated stress components from the matrix to the filler. The increase in the peak stress in the cenosphere due to the matrix relaxation is about 15%, as estimated by comparison with a linear elastic analysis.

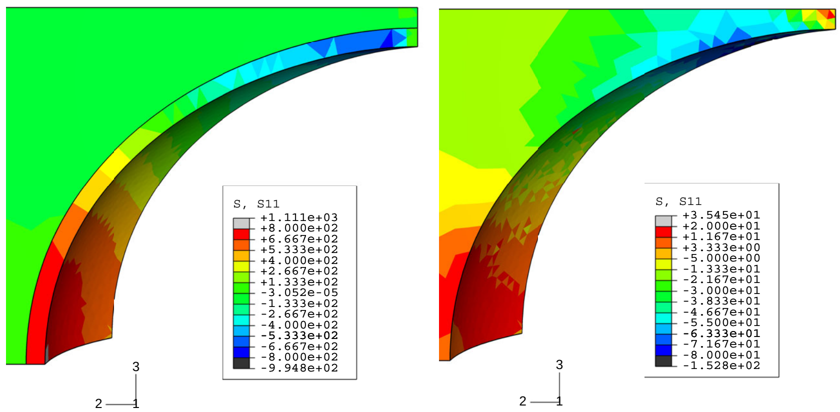

Figure 10. Three-dimensional unit cell model: the hoop stress contours at failure.

OPEN ISSUES AND CONCLUSIONS

The results here reported should be discussed at the light of not yet available data on the real distribution of defects in the fillers employed. Anyway, they clearly suggest that the relative stiffnesses of matrix and filler play a fundamental role in the failure modality of syntactic foams. Therefore, the radius ratio η as expressed by equation (1) should be a fundamental parameter to be considered together with the elastic moduli of matrix and cenosphere wall for a proper, advanced design of syntactic foams.

Moreover, since it appears that brittle failure may happen as micro-defects may propagate in the cenospheres, the filler size and gradation should also affect the ultimate behavior. By the way, the filler packing (dependent on its gradation and volume fraction) may also lead to a size effect in the matrix.

In order to try and understand the reasons for failure modalities different from the one analyzed here other ingredients, so far neglected, should be added to our

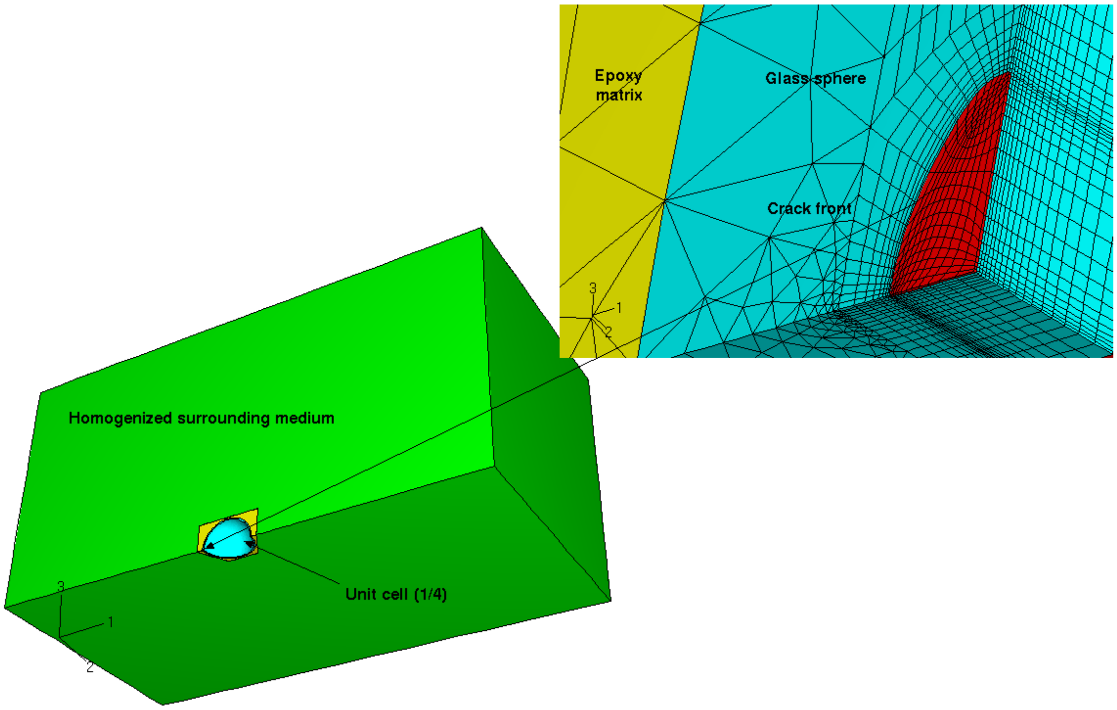

Figure 11. The Eshelby-like model.

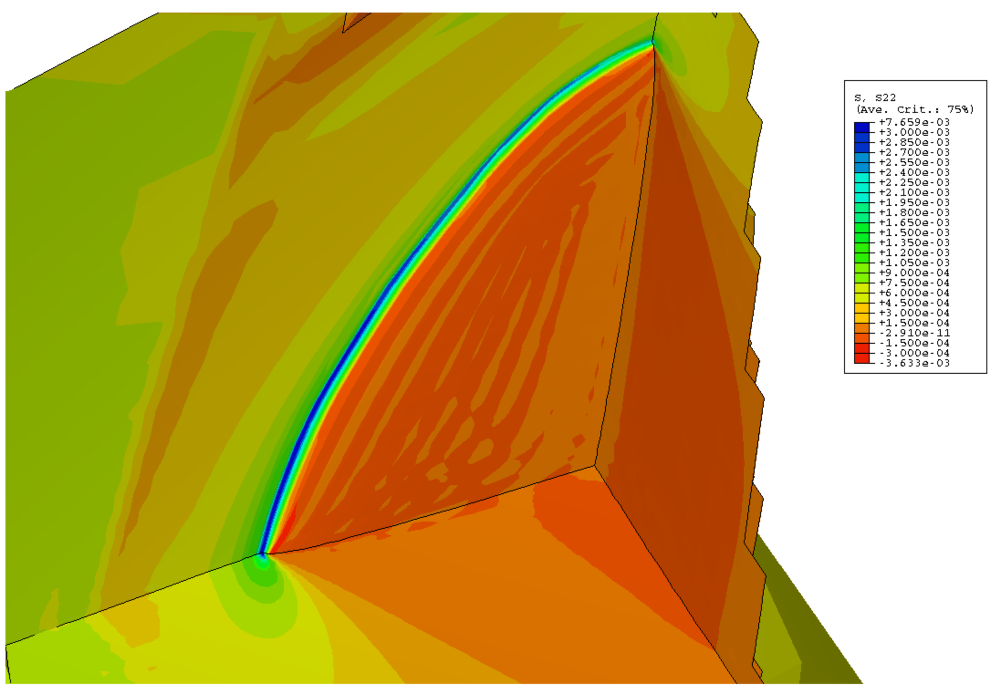

Figure 12. Syntactic foam type A: the hoop stress singularity on a flawed cenosphere.

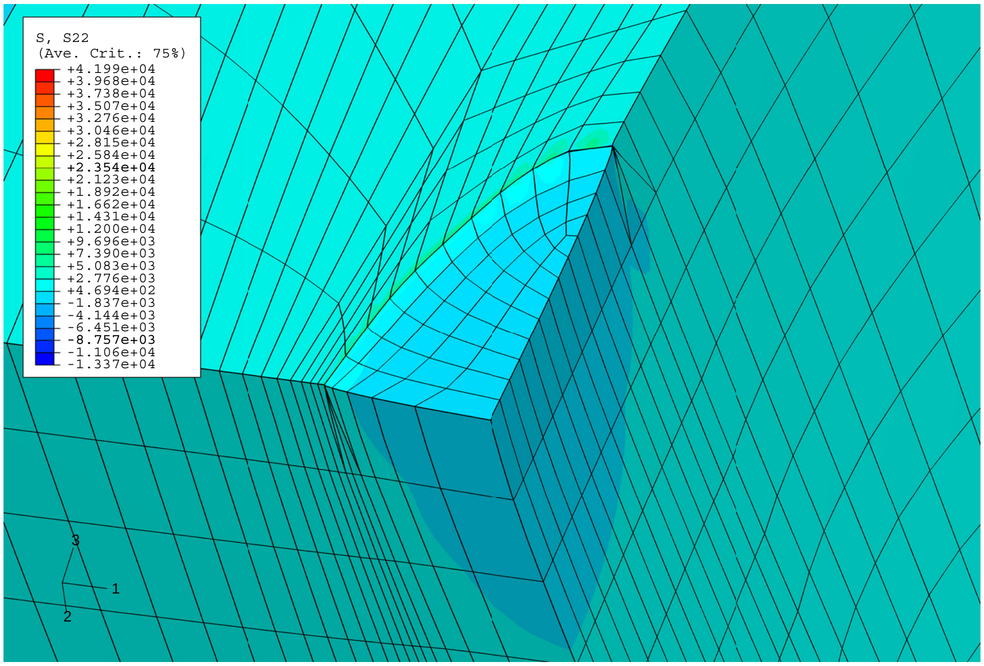

Figure 13. Contours and deformed shape for the model involving quarter-point elements.

model. First of all, the extension of the constitutive law for epoxy resins to account for viscoplastic deformations is under way. Then, we should remove the assumption of perfect adhesion between filler and matrix and adopt a mechanical law for the interface.

Nevertheless, even without these major improvements, the model employed so far should be useful to check at least which filler heaviness (i.e., η), for given materials and boundary conditions (i.e., imposed uniaxial displacement rate), discriminates between brittle failure type 1 and quasi-brittle failure type 2. Yet, this would require a noticeable load of experimental and numerical work.

ACKNOWLEDGMENTS

Work done within a research project financed by Italian Ministry of Education, University, and Research (MIUR).

The Finite Element code ABAQUS has been run at the Department of Civil Engineering, University of Brescia, Italy, under an academic license.

APPENDIX: Interface Conditions to Solve the Linear Elastic Problem on the Four–Phase Model

Here, we report the systems to be solved in order to compute the strain averages on each inclusion wall ($\overline{\varepsilon}_{12}^{(i),\lambda}$, $\overline{\vartheta}^{(i),\lambda}$), matrix shell ($\overline{\varepsilon}_{12}^{(m),\lambda}$, $\overline{\vartheta}^{(m),\lambda}$), and composite sphere ($\overline{\varepsilon}_{12}^{(c.s.),\lambda}$, $\overline{\vartheta}^{(c.s.),\lambda}$) needed to apply equations (2)–(3) and (7)–(8). All the details about the related boundary value problem are given in [5].

The following two systems, in the unknown coefficients I_1, I_2, I_3, I_4, M_1, M_2, M_3, M_4, S_2, and S_4 and J_1, J_2, P_1, P_2, and T_2 respectively, must be solved for each composite sphere λ, for $\lambda = 1, \dots, M$ (here, for simplicity, we omit the symbol λ and then the relevant radii become a, b, and c).

The first system (arising by applying simple shear boundary conditions to the four–phase model) reads:

$$2I_1 - 8I_2 + C_1^{(i)} I_3 + C_3^{(i)} I_4 = 0 \tag{10}$$

$$40I_2 + C_2^{(i)} I_3 + C_4^{(i)} I_4 = 0 \tag{11}$$

$$I_1 + \frac{a^5}{b^5} I_2 + \frac{b^2}{a^2} I_3 + \frac{a^3}{b^3} I_4 = M_1 + \frac{a^5}{b^5} M_2 + \frac{b^2}{a^2} M_3 + \frac{a^3}{b^3} M_4 \tag{12}$$

$$-5\frac{a^7}{b^7} I_2 + \alpha_2^{(i)} I_3 + (\alpha_{-3}^{(i)} - 5)\frac{a^5}{b^5} I_4 = -5\frac{a^7}{b^7} M_2 + \alpha_2^{(m)} M_3 + (\alpha_{-3}^{(m)} - 5)\frac{a^5}{b^5} M_4 \tag{13}$$

$$\begin{aligned} G^{(i)}\Big(2I_1 - 8\frac{a^5}{b^5} I_2 + C_1^{(i)} \frac{b^2}{a^2} I_3 + C_3^{(i)} \frac{a^3}{b^3} I_4\Big) = \\ = G^{(m)}\Big(2M_1 - 8\frac{a^5}{b^5} M_2 + C_1^{(m)} \frac{b^2}{a^2} M_3 + C_3^{(m)} \frac{a^3}{b^3} M_4\Big) \end{aligned} \tag{14}$$

$$G^{(i)}\Big(40\frac{a^7}{b^7} I_2 + C_2^{(i)} I_3 + C_4^{(i)} \frac{a^5}{b^5} I_4\Big) = G^{(m)}\Big(40\frac{a^7}{b^7} M_2 + C_2^{(m)} M_3 + C_4^{(m)} \frac{a^5}{b^5} M_4\Big) \tag{15}$$

$$M_1 + \frac{a^5}{c^5} M_2 + \frac{c^2}{a^2} M_3 + \frac{a^3}{c^3} M_4 = \Phi + \frac{a^5}{c^5} S_2 + \frac{a^3}{c^3} S_4 \tag{16}$$

$$-5\frac{a^7}{c^7} M_2 + \alpha_2^{(m)} M_3 + (\alpha_{-3}^{(m)} - 5)\frac{a^5}{c^5} M_4 = -5\frac{a^7}{c^7} S_2 + (\alpha_{-3}^{(s)} - 5)\frac{a^5}{c^5} S_4 \tag{17}$$

$$\begin{aligned} G^{(m)}\Big(2M_1 - 8\frac{a^5}{c^5} M_2 + C_1^{(m)} \frac{c^2}{a^2} M_3 + C_3^{(m)} \frac{a^3}{c^3} M_4\Big) = \\ = G^{(s)}\Big(2\Phi - 8\frac{a^5}{c^5} S_2 + C_3^{(s)} \frac{a^3}{c^3} S_4\Big) \end{aligned} \tag{18}$$

$$G^{(m)}\Big(40\frac{a^7}{c^7} M_2 + C_2^{(m)} M_3 + C_4^{(m)} \frac{a^5}{c^5} M_4\Big) = G^{(s)}\Big(40\frac{a^7}{c^7} S_2 + C_4^{(s)} \frac{a^5}{c^5} S_4\Big) \tag{19}$$

In all the preceding equations Φ represents a simple shear strain component applied to the unbounded medium surrounding each composite sphere and coefficients $\alpha_2^{(\zeta)}$, $\alpha_{-3}^{(\zeta)}$, $C_1^{(\zeta)}$, $C_2^{(\zeta)}$, $C_3^{(\zeta)}$ and $C_4^{(\zeta)}$ are defined as follows:

$$\alpha_2^{(\zeta)} = -2\frac{7 - 10\nu^{(\zeta)}}{7 - 4\nu^{(\zeta)}} \qquad \alpha_{-3}^{(\zeta)} = 2\frac{4 - 5\nu^{(\zeta)}}{1 - 2\nu^{(\zeta)}} \tag{20}$$

$$C_1^{(\zeta)} = \frac{14 + 4\nu^{(\zeta)}}{7 - 4\nu^{(\zeta)}} \qquad C_2^{(\zeta)} = 4\frac{7 - 4\nu^{(\zeta)} - (7 - 10\nu^{(\zeta)})(2 + \nu^{(\zeta)})}{(7 - 4\nu^{(\zeta)})(1 - 2\nu^{(\zeta)})} \tag{21}$$

$$C_3^{(\zeta)} = 2\frac{1 + \nu^{(\zeta)}}{1 - 2\nu^{(\zeta)}} \qquad C_4^{(\zeta)} = \frac{-24}{1 - 2\nu^{(\zeta)}} \tag{22}$$

where index ζ becomes i, m and s in the various regions of the four-phase model.

The second system (related to volumetric boundary conditions applied to the four–phase model) reads:

$$3K^{(i)} J_1 - 4G^{(i)} J_2 = 0 \tag{23}$$

$$3K^{(i)}J_1 - 4G^{(i)}J_2\frac{a^3}{b^3} = 3K^{(m)}P_1 - 4G^{(m)}P_2\frac{a^3}{b^3} \tag{24}$$

$$J_1 + J_2\frac{a^3}{b^3} = P_1 + P_2\frac{a^3}{b^3} \tag{25}$$

$$3K^{(m)}P_1 - 4G^{(m)}P_2\frac{a^3}{c^3} = 3K^{(s)}\Theta - 4G^{(s)}T_2\frac{a^3}{c^3} \tag{26}$$

$$P_1 + P_2\frac{a^3}{c^3} = \Theta + T_2\frac{a^3}{c^3} \tag{27}$$

$3\Theta = E_{kk}$ being the change of volume imposed on each considered four–phase model.

Finally,

$$\overline{\varepsilon}_{12}^{(m)} = M_1 + (1 + \frac{1}{5}\alpha_2^{(m)})\frac{c^5 - b^5}{a^2(c^3 - b^3)}M_3 \tag{28}$$

$$\overline{\varepsilon}_{12}^{(i)} = I_1 + (1 + \frac{1}{5}\alpha_2^{(i)})\frac{a^4 + a^3b + a^2b^2 + ab^3 + b^4}{a^2(a^2 + ab + b^2)}I_3 \tag{29}$$

$$\overline{\varepsilon}_{12}^{(c.s.)} = M_1 + (1 + \frac{1}{5}\alpha_2^{(m)})\frac{c^2}{a^2}M_3 + \frac{1}{5}\alpha_{-3}^{(m)}\frac{a^3}{c^3}M_4 \tag{30}$$

$$\overline{\vartheta}^{(m)} = P_1 \tag{31}$$

$$\overline{\vartheta}^{(i)} = J_1 \tag{32}$$

$$\overline{\vartheta}^{(c.s.)} = P_1 + P_2\frac{a^3}{c^3} \tag{33}$$

REFERENCES

1. Shutov, F.A. 1986. "Syntactic polymer foams," *Advances in Polymer Science*, 73/74:63-123.

2. Gupta, N., E. Woldesenbet, and P. Mensah. 2004. "Compression properties of syntactic foams: effect of cenosphere radius ratio and specimen aspect ratio," *Composites: Part A*, 35:103-111.

3. Bardella, L. and F. Genna. 2001. "On the elastic behavior of syntactic foams," *International Journal of Solids and Structures*, 38(40-41):7235-7260.

4. De Runtz, J.A.Jr and O. Hoffman. 1969. "The static strength of syntactic foams," *Journal of Applied Mechanics*, 36(E4):551-557.

5. Bardella, L. 2000. "Mechanical behavior of glass-filled epoxy resins: experiments, homogenization methods for syntactic foams, and applications," Ph.D. thesis, Department of Civil Engineering, University of Brescia, Italy. http://192.167.21.48/utenti/bardella/thesis.pdf

6. Rizzi, E., E. Papa, and A. Corigliano. 2000. "Mechanical behavior of a syntactic foam: experiments and modeling," *International Journal of Solids and Structures*, 37:5773-5794.

7. Bardella, L. 2001. "A phenomenological constitutive law for the nonlinear viscoelastic behaviour of epoxy resins in the glassy state", *European Journal of Mechanics A/Solids*, 20(6):907-924.

8. Bardella, L. 2003. "An extension of the Secant Method for the homogenization of the nonlinear behavior of composite materials," *International Journal of Engineering Science*, 41:741-768.

9. Bornert, M., C. Stolz, and A. Zaoui. 1996. "Morphologically Representative Pattern-based bounding in elasticity," *Journal of the Mechanics and Physics of Solids*, 44:307-331.

10. Hashin, Z. 1962. "The elastic moduli of heterogeneous materials," *Journal of Applied Mechanics*, 29:143-150.

11. Hervé, É. and O. Pellegrini. 1995. "The Elastic Constants of a Material Containing Spherical Coated Holes," *Archives Mechanics*, 47(2):223-246.

12. 3M Italia. 1993. "Scotchlite^{TM} Glass Bubbles. Informazioni di prodotto," (in Italian), private communication.

13. Suquet, P. 1997. "Effective properties of nonlinear composites," in *Continuum Micromechanics. CISM Lecture Notes 377*, P. Suquet, ed. Wien:Springer-Verlag, pp. 197-264.

14. Al-Moussawi, H., E.D. Drown, and L.T. Drzal. 1993. "The silane/sizing composite interphase," *Polymer Composites*, 14(3):195-200.

15. d'Almeida, J.R.M. 1999. "An analysis of the effect of the diameters of glass microspheres on the mechanical behavior of glass-microsphere/epoxy-matrix composites," *Composites Science and Technology*, 59:2087-2091.

16. Gupta, N. and E. Woldesenbet. 2004. "Microballoon wall thickness effects on properties of syntactic foams," *Journal of Cellular Plastics*, 40:461-479.

17. Maier, G. 1998. "Analisi delle proprietà chimiche, fisiche e micromeccaniche di un materiale composito in sandwich di schiuma sintattica e fibra di vetro preimpregnata. Studio del comportamento meccanico di un materiale composito a sandwich di schiuma sintattica e fibra di vetro," (in Italian), Internal report, private communication.

18. Eyring, H. 1936. "Viscosity, plasticity and diffusion as examples of absolute reaction rates," *Journal of Chemistry and Physics*, 4:283-291.

19. Oleinik, E.F. 1986. "Epoxy-aromatic amine networks in the glassy state: structures and properties," *Advances in Polymer Science*, 80:49-99.

20. Hibbitt, Karlsson & Sorensen, Inc. 2001. *ABAQUS User's & Theory Manuals, Release 6.1*, Pawtucket, USA.

21. Wei, D., D. Baptiste, Ph. Bompard, and D. François. 1989. "A damage micromechanics approach to a heterogeneous material," in *Cracking and Damage, Strain Localization and Size Effect*, J. Mazars and Z.P. Bažant, eds. New York:Elsevier, pp. 128-139.

22. Ashby, M.F. 1989. "On the engineering properties of materials," *Acta Metallurgica*, 37(5):1273-1293.